

# RESEARCH ARTICLE

# Toxic Dye Degradation Employing *Phoenix dactylifera* Seed Extract for the Green Synthesis of Silver Nanoparticles: Characterization and Application

<sup>1</sup>Department of Chemistry, Forman Christian College (A Chartered University), Lahore, Pakistan | <sup>2</sup>Biomedical Engineering Department, College of Engineering and Technologies, Al-Mustaqbal University, Babylon, Iraq | <sup>3</sup>Nanomaterials Research Center, Department of Chemistry, College of Science, Mathematics, and Technology, Wenzhou-Kean University, Wenzhou, Zhejiang, China | <sup>4</sup>Dorothy and George Hennings College of Science, Mathematics and Technology, Kean University, Union, New Jersey, USA | <sup>5</sup>Nottingham Ningbo China Beacons of Excellence Research and Innovation Institute, University of Nottingham Ningbo China, Ningbo, China | <sup>6</sup>Functional Materials Group, Gulf University for Science and Technology, Mishref, Kuwait | <sup>7</sup>Department of Biotechnology, College of Science, Taif University, Taif, Saudi Arabia

Correspondence: Shahid Iqbal (mshahidiqbal@hzu.edu.cn) | Sajid Mahmood (sajidmahmood1987@yahoo.com)

Received: 31 August 2024 | Revised: 4 November 2024 | Accepted: 12 November 2024

Review Editor: Mingying Yang

Funding: This work was supported by Taif University, TU-DSPP-2024-65.

**Keywords:** AgNPs | dyes | green synthesis | *Phoenix dactylifera* | photocatalytic degradation

# **ABSTRACT**

This research highlights the facile green synthesis of silver nanoparticles (AgNPs) using *Phoenix dactylifera* seed extracts and its photocatalytic application for the degradation of toxic dyes. The AgNPs synthesis was confirmed by the appearance of its representative absorption peak at 416 nm in UV-visible absorption spectroscopy. Moreover, the reduction of silver ions to Ag was justified through Fourier transform infrared (FTIR) spectroscopy. X-ray diffraction pattern revealed crystalline AgNPs structure with particle size ranging from 5 to 15 nm calculated using the Debye–Scherrer equation. The rectangular-like structural morphology of synthesized AgNPs was observed in scanning electron micrographs. The as-synthesized AgNPs demonstrated higher photocatalytic activity for the degradation of malachite green (MG) and congo red (CR) followed by methylene blue (MB), and crystal violet (CV) under UV irradiation. In addition, rate constant (k) and percentage degradation were also calculated. The present study presents a facile green synthesis pathway and its potentially successful manipulation in the reduction of toxic dyes under the illumination of UV-light.

# 1 | Introduction

The date palm, or *Phoenix dactylifera* L., is a member of the Aceraceae family and is among the first known agricultural plants, having been domesticated between 5500 and 3000 BCE. For over 1400 years, *P. dactylifera* products have been a staple in the diets of Islamic countries. The "Ajwa" variety, prevalent

in Arab nations, has been extensively studied and utilized for its medicinal and pharmacological benefits (Liu et al. 2018). Ajwa date seeds are rich in proteins and crude fat, and they also contain significant amounts of total dietary fiber (TDF), They contain not only soluble dietary fiber (SDF) but also insoluble dietary fiber (IDF) content (Liu et al. 2020). Products derived from *P. dactylifera*, including its fruits, seeds, pollen, leaves, and

Areesha Maryam and Saqib Rabbani are joint first authors and equally contributed to this study.

© 2024 Wiley Periodicals LLC.

# **Summary**

- The facile green construction of nanoparticles of silver (AgNPs) using the extract of *Phoenix dactylifera*.
- XRD revealed crystalline AgNP structure with particle size ranging from 5 to 15 nm calculated using the Scherrer equation.
- The stability of bio-reduced AgNPs was analyzed using UV-spectroscopy.
- Results showed that AgNPs were stable even after 1 month.
- FTIR unfolded the functional groups responsible for reducing Ag<sup>+</sup> to AgNPs.

syrup, offer numerous benefits for both humans and animals (Zeng et al. 2020). The protective properties of *P. dactylifera* are thought to arise not only from its fiber, vitamins, and minerals but also from a wide array of plant secondary metabolites. The Ajwa date is abundant in phytochemicals like polyphenols, flavonoids, isoflavonoids, sterols, and lignin, all of which have effectively decreased blood cholesterol l and reduced the chances of cardiovascular problems. Moreover, the polyphenolic proanthocyanidins, in conjunction with other phenolics, may act as free radical scavengers or heavy metal chelators, thereby helping to alleviate oxidative stress and inflammation (Zhang et al. 2018).

Nanotechnology is a diverse scientific domain that includes almost all scientific disciplines that is chemistry, physics, biology, colloidal science, and so forth for investigating materials at the nanoscale level (Shi et al. 2022). Recent advances in nanotechnology have unfolded many new research horizons in materials science. Nanotechnology-aided research in biotechnology (Munir et al. 2020), analytical science (Iqbal and Iqbal 2013), quantum dots (Bahadur et al. 2018), microbiology, (Bahadur et al. 2021) and many other disciplines, have paved the way for solving many critical problems and are vitally important in new technologies such as mechanics, optics (Irfan et al. 2021), biomedical sciences (Chan et al. 2017), chemical industry (Irfan et al. 2020; Hussain et al. 2019), optoelectronic devices (Abubshait et al. 2021), drug delivery (Saeedi et al. 2019), and photoelectrochemical applications (Iravani 2011). Nanoparticles are highly valued because of their exceptionally small size, and they also possess a large surface-to-volume ratio, which results in significant physical and chemical differences from their bulk counterparts of similar chemical configurations. These differences manifest in various properties, such as biological integrity, mechanical strength, steric behavior, melting point catalytic activity, thermal stability, optical absorption, and electrical conductivity (Iravani 2011; Li et al. 2018).

In the past decade, metal nanoparticles (MNPs) have garnered significant attention due to their unique properties particularly size and surface area, optical, electronic, sensing, catalytic, and antibacterial characteristics (Shoaib et al. 2021). Out of all noble metals, silver nanoparticles (AgNPs) stand out as a versatile element, historically used in the creation of coins and jewelry (Hambardzumyan et al. 2020). Silver nanoparticles are

primarily utilized in glassware, electric batteries, and ceramic pigments, as well as in medical devices for treating diseases such as HIV, cancer, diabetes, tuberculosis, and malaria (Ur Rahman et al. 2020). AgNPs also possess catalytic properties and can detect biological molecules. Currently, their applications in biolabeling and optical sensing are being extensively explored (Hamedi and Shojaosadati 2019). Various chemical methods have been developed for synthesizing nanoparticles, many of which are commonly used to produce nanostructured materials. These methods include pyrolysis, chemical reduction, solgel processing, microemulsion, hydrothermal synthesis, polyol synthesis, physicochemical processes, chemical vapor deposition, electrochemical techniques, sonochemical methods, thermal decomposition, microwave-assisted synthesis, solvothermal approaches, photochemical reduction, photosynthesis, and continuous-flow methods (Hambardzumyan et al. 2020; Muthu and Priya 2017; Patil and Chandrasekaran 2020). Additionally, traditional chemical synthesis of MNPs is often energy-intensive and involves hazardous chemicals and reagents. The byproducts generated during these processes can be harmful to humans and detrimental to the environment. Consequently, the use of these nanoparticles is often restricted in biological applications (Khodadadi, Bordbar, and Nasrollahzadeh 2017).

Green synthesis of AgNPs offers several advantages such as it is a cost-effective, convenient single-step process and eco-friendly. This method does not require high pressure, harsh temperature conditions, or lethal chemicals, making it a more sustainable alternative (Robinson et al. 2020). Many scientists have stated the plant-mediated green synthesis of silver nanoparticles using various plants and their extracts from different parts of the plant, including roots (Behravan et al. 2019), stem (Uddin et al. 2021), bark (Burlacu et al. 2019), leaf (Goutam et al. 2018), fruit (Jayaprakash et al. 2017), bud (Lakhan et al. 2020), and latex (Kalaiselvi et al. 2019) as natural resources. The extracts from these plant parts contain various biomolecules, that help to reduce metal ions and stabilize nanoparticles, helping to achieve the desired shapes and sizes (Modi 2018; Jyoti and Singh 2016). In various studies, a huge number of medicinal plants such as Ocimum tenuiflorum (Singh et al. 2018), Cassia auriculata (Muthu and Priya 2017), Pulicaria glutinosa (Tahir et al. 2013), Diospyros lotus (Hamedi and Shojaosadati 2019), Ananas comosus (Ahmad and Sharma 2012), P. dactylifera (Farhadi, Ajerloo, and Mohammadi 2017), Capsicum annuum (Li et al. 2007), Argemone mexicana (Singh et al. 2010), Olea europaea (Khalil et al. 2014), and many more have already been used to synthesize and stabilize metallic NPs, particularly biogenic AgNPs.

Dyes are synthetic organic compounds used for versatile applications (Habibi and Askari 2011). The textile industry uses a substantial number of synthetic dyes, accounting for about 60% of total dye production, to enhance the appearance and texture of fabrics. Additionally, approximately 15% of these dyes are wasted after their intended use (Gonawala and Mehta 2014). These dye compounds dissolve in water bodies at concentrations ranging from 10 to 200 mg/L, leading to substantial water pollution on a global scale (Jyoti and Singh 2016). Therefore, treating dye effluents from textile industries is essential for wastewater management. Since the hue of these effluents lowers sunlight penetration and dissolved oxygen in water bodies, their discharge into aquatic systems presents serious

environmental problems. Additionally, it can release toxic compounds through chemical or biological reactions, adversely affecting aquatic flora and fauna. Traditional physical–chemical and biological methods for reducing dye compounds are often ineffective, time-consuming, and challenging, especially at high effluent concentrations. In contrast, reductive degradation of dyes using nanomaterials offers a more promising solution due to their unique physicochemical properties (Sharma et al. 2018).

Hence, in this paper, AgNPs have been synthesized by the green and environmentally benign method using *P. dactylifera* seed extract as reducing-cum-stabilizing agent and investigated their photocatalytic activity for degradation of hazardous dyes (Figure 1) that is malachite green (MG), methylene blue (MB), congo red (CR), and crystal violet (CV) under the exposure of UV light.

# 2 | Materials and Methods

# 2.1 | Reagents

Silver nitrite ( ${\rm AgNO_3}$ ) was procured from Sigma-Aldrich Germany. MB, CV, and MG were purchased from Merck Germany, whereas CR was purchased from Riedel-de Haën. Furthermore, deionized water (DI) was used for the synthesis of AgNPs.

# 2.2 | Procedure

# 2.2.1 | Preparation of Ajwa Seed Powder

Ajwa date seed extract (from *P. dactylifera*) was utilized as both a reducing and stabilizing agent. The dates were purchased from Lahore, Pakistan, where they are commercially available. The seeds were carefully separated and washed multiple times with DI. After washing, the seeds were weighed and dried overnight in an oven at 60°C. Once dried, the seeds of the Ajwa were

ground to a fine powder using industrial-grade steel mortar and pestle.

#### 2.2.2 | Preparation of Ajwa Aqueous Extract

Aqueous extract of *P. dactylifera* was prepared by taking 2g powdered Ajwa seeds in 100 mL distilled water and kept soaked for 24 h. The Ajwa seeds extract was filtered and the filtrate was stored at 4°C for the synthesis of AgNPs.

# 2.2.3 | Green Synthesis of Silver Nanoparticles

AgNPs were synthesized by combining  $5\,\mathrm{mL}$  of  $5\,\mathrm{mM}$  AgNO $_3$  with  $0.5\,\mathrm{mL}$  of Ajwa aqueous extract in a  $25\,\mathrm{mL}$  beaker and it is diluted to achieve a total volume of  $10\,\mathrm{mL}$ . The solution was stirred for  $2\,\mathrm{h}$  to ensure it became homogeneous. After this period, the yellow color of the solution was changed to brown, indicating the successful formation of colloidal AgNPs.

# 2.2.4 | Photocatalytic Degradation and Kinetic Studies

The photocatalytic activity of the newly synthesized AgNPs has been investigated by exposing 50 mL of suspension containing 15 ppm MG dye and 0.05 g AgNPs to UV-light. Prior to the light exposure, the mixture was stirred magnetically and kept in the dark for 30 min. The sample was then collected with syringe filter after a regular interval of 10 min. The photodegradation of the MG dye was monitored by recording absorption spectra using UV-visible spectrophotometer. Moreover, the percentage degradation of the MG dye was determined using the given equation (Raj et al. 2020):

% Degradation = 
$$\left(\frac{A_0 - A_t}{A_0}\right) \times 100$$
 (1)

where  $A_0$  and  $A_t$  are the absorption of the sample at time zero and any time "t". Furthermore, kinetic study was investigated

FIGURE 1 | Structure of (a) malachite green, (b) congo red, (c) methylene blue, and (d) crystal violet dyes.

by assessing the validity of pseudo first and second order kinetic models, and subsequent rate constants were estimated from the slope of the following linear equations (Raj et al. 2020):

$$\ln(A_o/A_t) = kt \tag{2}$$

$$\frac{1}{A_t} = kt + \frac{1}{A_0} \tag{3}$$

Moreover, similar procedure was adopted to study the % degradation and kinetics of MB, CR, and CV dyes by the as synthesized AgNPs in the illumination of UV light.

# 3 | Results and Discussion

# 3.1 | Phytoreduction of Silver

In this investigation, phytosynthesis of AgNPs by seed extract of date palm (aqueous medium) was studied. It was noticed that the mixture of silver nitrate and the date seed extract exhibited a major color change from yellow to brown within the first 30 min while stirring for 2h. Subsequently, no further change was observed. This can be attributed to the formation of AgNPs due to the reduction of Ag+ into Ag by the phytochemicals present in the extract. Whereas, no any color change was observed in the AgNO<sub>3</sub> solution without date seed extract. Brown color appearance can also be attributed to surface plasmon resonance (SPR) vibrations in AgNPs (Ahmed et al. 2016).

# 3.2 | UV-Visible Analysis

UV-Vis spectroscopy, is an important technique for investigating the synthesis of AgNPs (Huang et al. 2008). It was used to characterize the formation of AgNPs from the silver salt and date seed extract solution. Various physiochemical parameters, including concentration of date seed extract and the salt, temperature conditions, and time of reaction, were adjusted to reduce Ag+ ions to AgNPs using date seed extract. To optimize the various concentrations of silver nitrate, its different solutions (2-5 mM AgNO<sub>3</sub>) were reacted with 1 mL date extract. Figure 2 shows the UV-Visible absorption spectra of AgNPs acquired at different concentrations (2, 3, 4, and 5 mM) AgNO<sub>3</sub>. At 2 mM, a clear SPR band figured, indicating a low yield of AgNPs formed, but with the increase in the concentration of NPs to 5 mM, the SPR of AgNPs shifted to 426 nm as represented in Figure 2. This happening may be attributed to the relatively fast growth of the particles at higher concentrations. At higher concentrations of AgNO<sub>3</sub>, the red-shifted band indicates the formation of larger particles (Ahmed et al. 2016). The AgNPs yield was observed increased with increasing concentration of AgNO<sub>3</sub> (2-5 mM) and the major yield was procured with 5 mM, which was hence used for further investigations.

Furthermore, the effect of varying the volume of date seed extract from 0.2 to  $2\,\mathrm{mL}$  on the synthesis of AgNPs was also investigated. A steady increase in the intensity of the typical surface plasmon resonance absorption band for AgNPs up to  $1.2\,\mathrm{mL}$  was observed as shown in Figure 3. Beyond this point, a broad SPR absorption band was observed and the maximum absorption occurred with

a 2 mL volume of date seed extract. The comparison of absorption spectra shown in Figure 3 indicates a change in wavelength from 423 to 448 nm, signifying a redshift as extract concentration rose from 0.2 to 2 mL. This indicates an increase in AgNPs size while increasing the amount of date seed extract.

Figure 4 presents the effect of reaction temperature 303.15, 313.15, and 323.15K on the synthesis of AgNPs. The comparison of spectra shows that initially absorption peak was shifted to higher wavelength with increasing temperature from 303.15 to 313.15 K. But at higher temperatures (323.15 K), a lower  $\lambda_{\text{max}}$  value was noticed which can be attributed to the formation of smaller AgNPs (Zia et al. 2016). The optimized reaction conditions were determined to be 0.5 mL of date seed extract, 5 mM AgNO, solution and 323.15 K reaction temperature. The observed broadening and redshift in the absorption peak are attributed to agglomeration or an increase in particle size. The similar shifts were also noticed in a previous study (Ndikau et al. 2017). After 30 min of reaction time, 323.15 K was found to be the ideal temperature for finishing the reaction. According to published research, raising the temperature to 80°C accelerates the pace at which silver ions are reduced (Amin et al. 2012). Hence, the NPs absorption has lot of information related to the particle size and aggregation (Philip 2010). Moreover, the inset of Figure 4 presents the bandgap energy (~2.4eV) of Ag NPs estimated from the tauc plot.

# 3.3 | XRD Analysis

The XRD pattern of AgNPs after a 10-min incubation period tells a face-centered cubic structure. As shown in Figure 5, the XRD configuration of the dried NPs suggests that they are crystalline. According to the JCPDS card number 04-0783, the broad diffraction peaks detected in the  $2\theta$  range of  $20^\circ-80^\circ$  at  $38.73^\circ$ ,  $46.69^\circ$ ,  $64.93^\circ$ , and  $77.81^\circ$  relate to the (111), (200), (220), and (311) planes, correspondingly. These XRD patterns confirm the synthesis of pure silver nanoparticles and are consistent with previously reported data (Kumar, Palanichamy, and Roopan 2014; Kumar et al. 2012). The average crystallite size was calculated using following Debye–Scherrer equation:

$$D = \frac{k \lambda}{\beta \cos \theta} \tag{4}$$

where D represents the average size of the nanoparticle crystals, k denotes the geometric constant (0.9),  $\lambda$  indicates the wavelength of the x-ray radiation source, and  $\beta$  represents full width at half maximum (FWHM) of the XRD preferred peak at  $2\theta$  diffraction angle (Balaji, Senthilkumaran, and Thangadurai 2014). The average crystallite size of the AgNPs calculated using Equation (4) was ~15 nm.

# 3.4 | SEM Analysis

Figure 6 presents the SEM images of the Ag NPs which were recorded at 10,000× and 20,000× magnifications with a working distance of 5.1 mm to consider the various aspects of the morphology of prepared nanoparticles such as size and texture. The prepared nanoparticles are observed rectangular in micrographs, which are distributed with smooth surfaces and

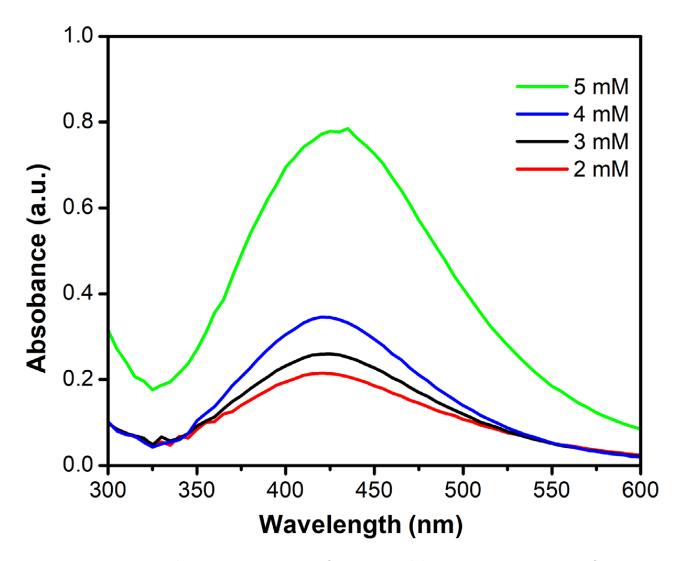


**FIGURE 2** | The comparison of UV–visible measurements of Ag NPs for various contents of AgNO $_3$ .

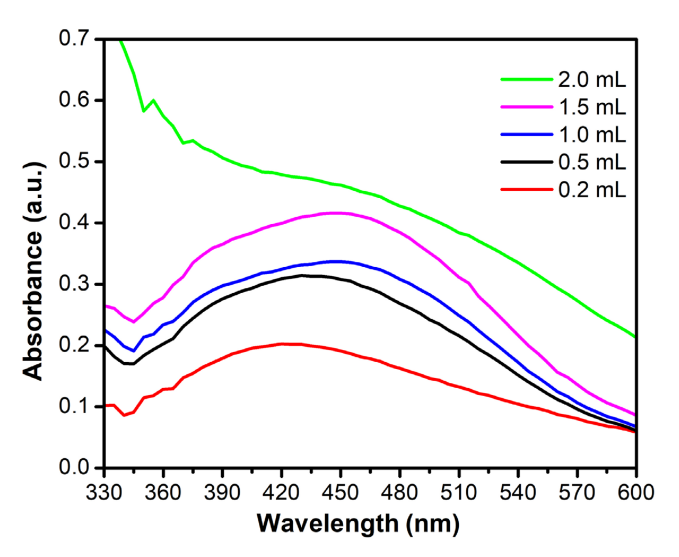


**FIGURE 3** | The comparison of UV-visible absorption spectra of Ag NPs prepared from  $5\,\mathrm{mM}$  AgNO $_3$  with varying volumes of date seed extract.

compact structures. The nanoparticles tend to form clusters because of their minor size and high surface energy. Moreover, particles with variable diameter can be seen in the SEM images.

# 3.4.1 | FTIR Analysis

FTIR spectroscopy was used to identify the potential biomolecules from *P. dactylifera* involved in the synthesis of AgNPs and it also plays a substantial function in the stabilization of NPs. Typically, pure silver nanoparticles exhibit weak IR absorption due to silver's minimal interaction with IR radiation. The FTIR spectrum (Figure 7) displayed peaks at 3271 and  $1642\,\mathrm{cm^{-1}}$ , which may correspond to O—H, aliphatic C—H, and carbonyl stretching vibrations of flavonoids or phenolic groups. Specifically, OH stretching of phenolic groups is depicted at  $3271\,\mathrm{cm^{-1}}$ , while at  $1734\,\mathrm{cm^{-1}}$  is likely associated with the C=O stretching of proteins, consistent with literature findings

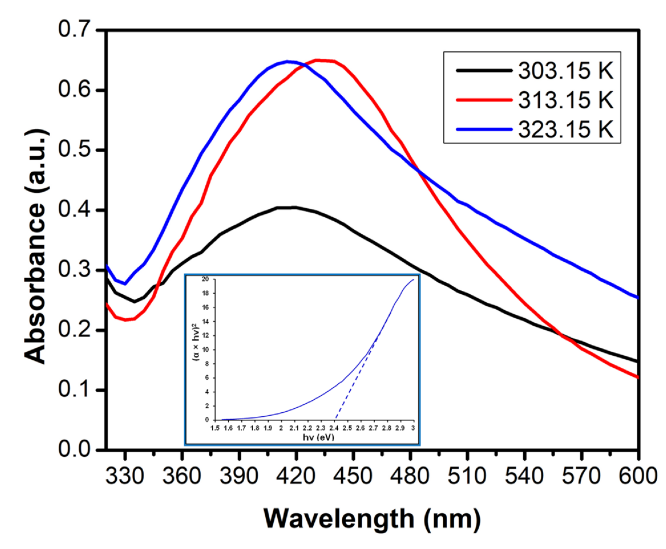


**FIGURE 4** | The comparison of UV-visible absorption spectra of Ag NPs prepared at different temperatures (K) from  $5\,\mathrm{mM}$  AgNO $_3$  and  $0.5\,\mathrm{mL}$  date seed extract whereas inset is the direct bandgap energy evaluation of Ag NPs prepared at  $323.15\,\mathrm{K}$ .

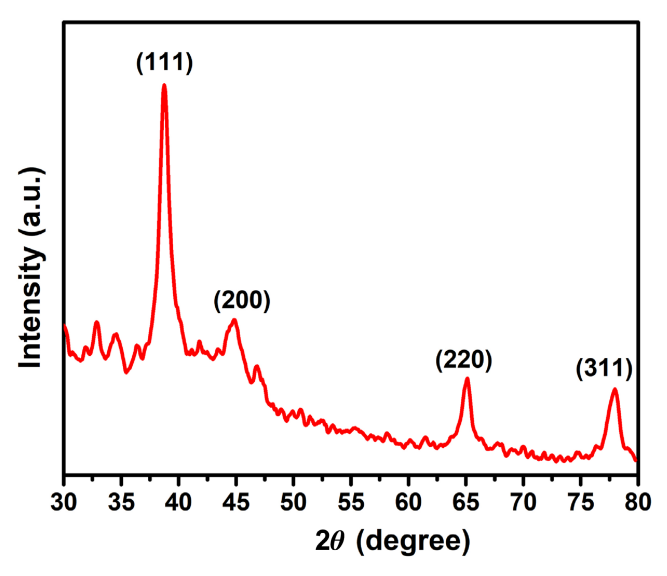


**FIGURE 5** | The x-ray diffraction pattern of Ag NPs prepared from date seed extract.

(Bobbu et al. 2016). FTIR analysis identified proteins, terpenoids (Mashwani et al. 2016), and flavonoids (Jain and Mehata 2017) in the aqueous seed extract of *P. dactylifera*. Flavonoids and terpenoids are likely involved in the synthesis of AgNPs, while proteins may contribute to their stabilization by coating the nanoparticles (Kumar et al. 2017). A shift in the peaks for AgNPs to 3275 and 1634 cm<sup>-1</sup> indicates that O—H and CO groups have adsorbed onto the surface of the nanoparticles, suggesting their involvement in the reduction process (Kumar et al. 2018).

# 3.5 | Photocatalytic Degradation of Dyes by the Ag NPs

Figure 8 presents a decrease in absorption of dyes in the presence of Ag NPs while increasing the UV light exposure duration. This

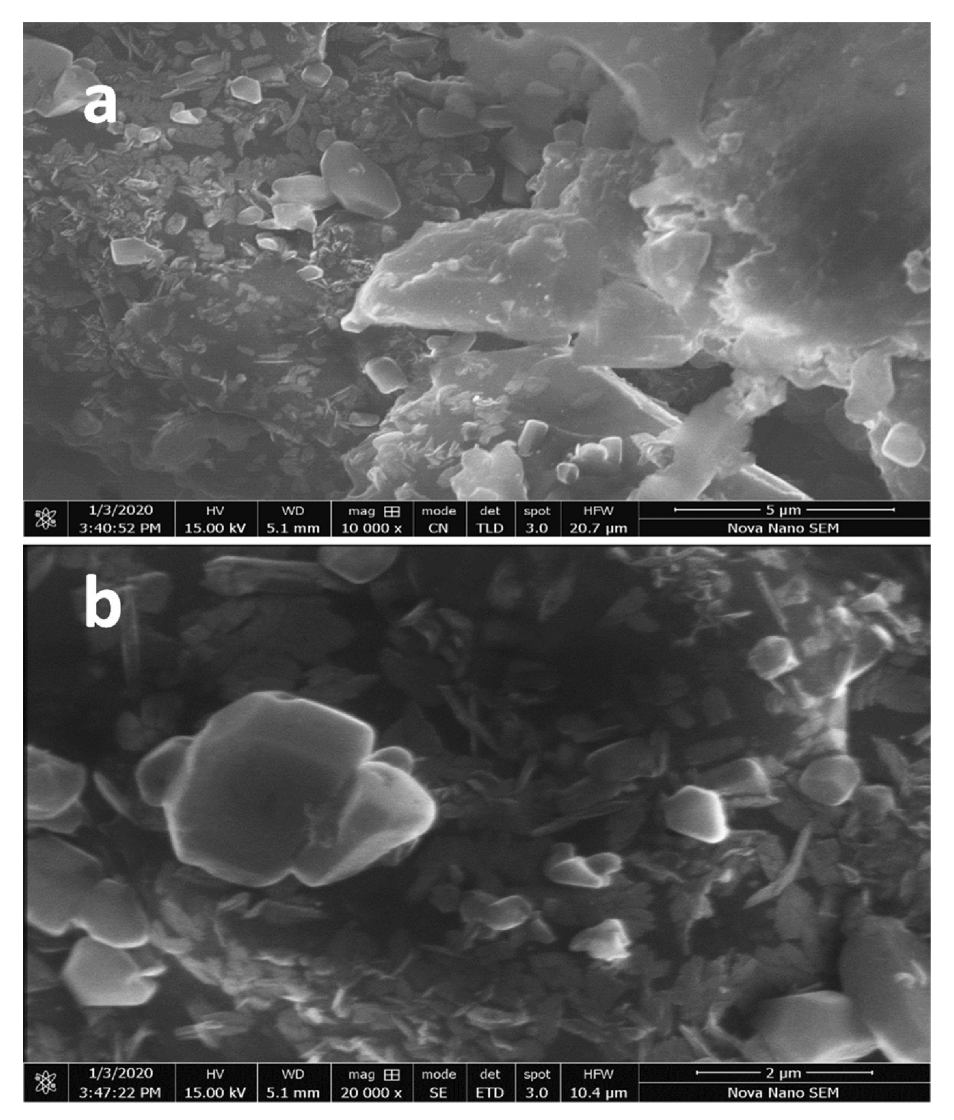


**FIGURE 6** | (a, b) SEM images of AgNPs at different magnifications.

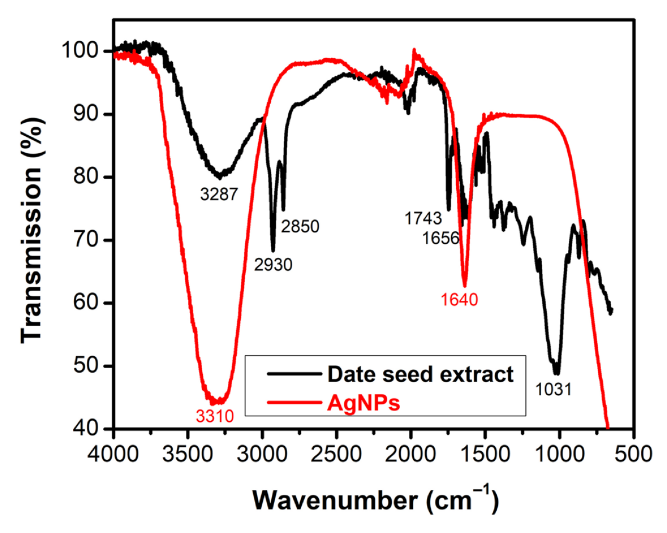


FIGURE 7 | The FT-IR spectra of AgNPs and date seed extract.

continuous decrease in the absorption of dyes also represents the involvement of Ag NPs in removing the dyes from the polluted water under light illumination. MG dye is characterized by a

specific wavelength of 620 nm as shown in Figure 8a wherein a steady drop in the dye solution's absorbance was observed which further suggests ~83% MB dye degradation through MB chromophore's breakage and then dye decolorization. Moreover, Figure 8b-d also present their successive degradation by AgNPs photocatalyst with increasing light exposure duration. The higher photodegradation of MG dye (Figure 9) by the AgNPs is mainly attributed to the dye's greater structural compatibility in terms of adsorption and interaction with the photocatalyst as compared to other dyes. The decreasing order of photodegradation of dyes is as follows:

Malachite green (83%) > Congo red (79%) > Crystal violet (62%) > Methylene blue (48%)

Kinetic studies revealed the validity of pseudo 1st order kinetic model with greater correlation coefficient than pseudo 2nd order kinetics for the photodegradation of all four dyes as shown in Figure 10. Moreover, the photodegradation through 1st order kinetics shows the breakage of dye structure initiated by its adsorption on the surface of a photocatalyst. In addition, the higher rate constant  $(8.2 \times 10^{-3} \, \mathrm{min}^{-1})$  for the degradation of

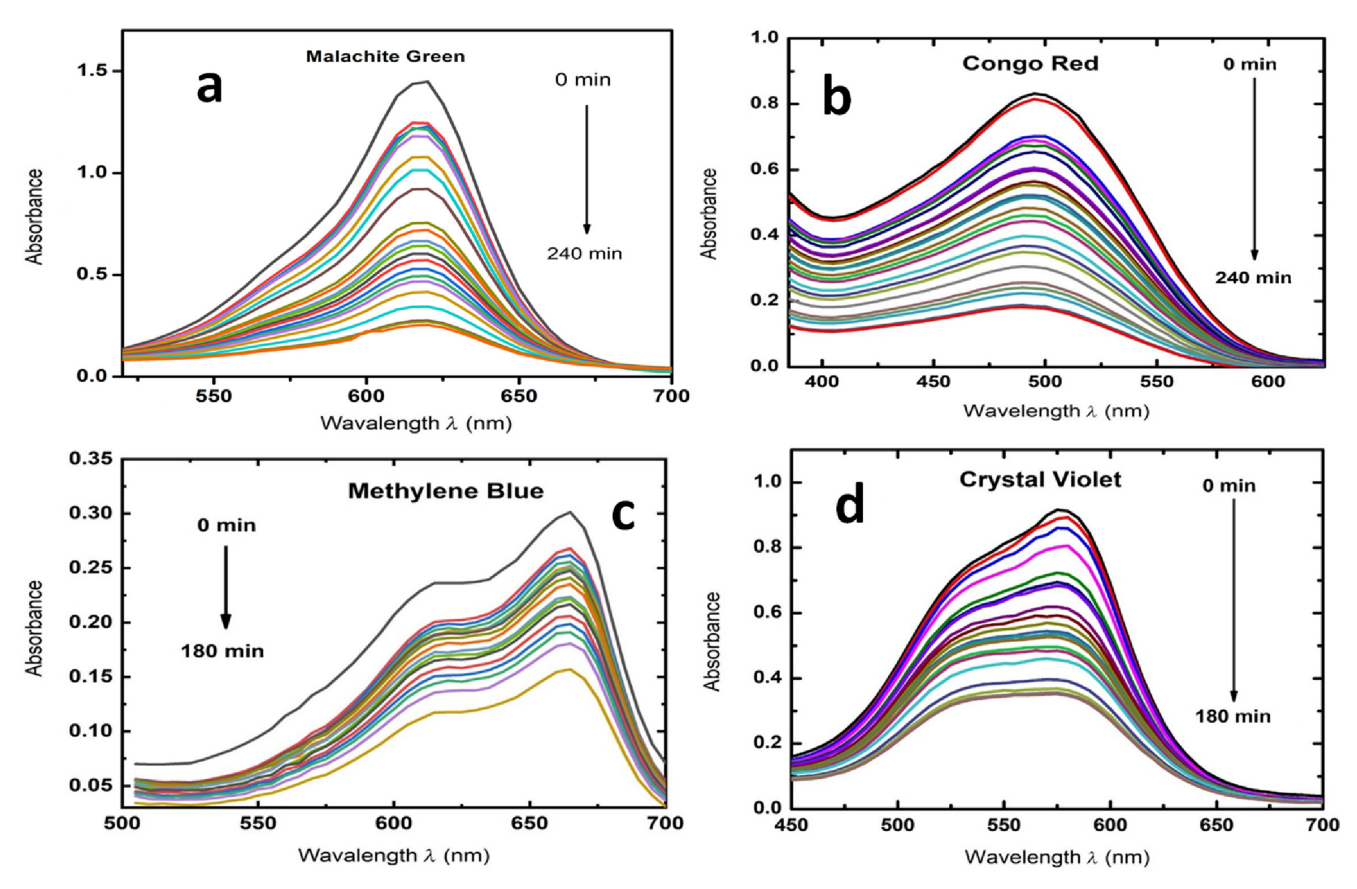
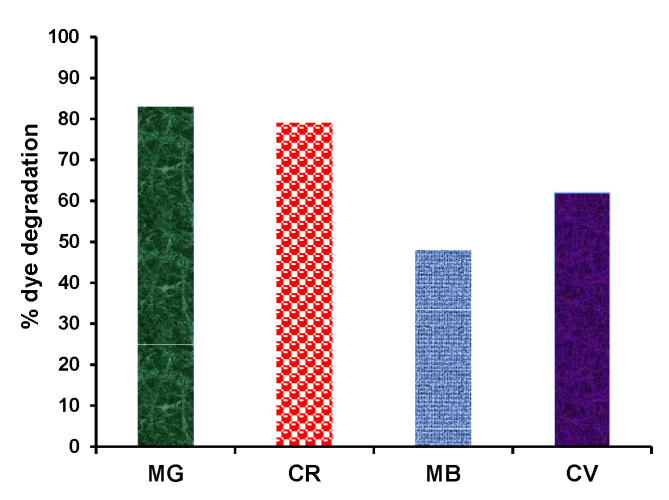


FIGURE 8 | The comparison of absorption spectra of (a) MG, (b) CR, (c) MB, and (d) CV dyes in the presence of Ag NPs at ambient temperature by increasing UV light exposure duration.



**FIGURE 9**  $\mid$  The comparison of % degradation of dyes by Ag NPs under the exposure of UV light.

MG dye indicates the fast MG adsorption and its structure compatibility with the surface of Ag NPs.

The decreasing trend of dye degradation rate over Ag NPs is provided below: MG  $(8.2 \times 10^{-3} \, \text{min}^{-1}) > \text{CR} \ (6.0 \times 10^{-3} \, \text{min}^{-1}) > \text{MB} \ (5.4 \times 10^{-3} \, \text{min}^{-1}) > \text{CV} \ (3.4 \times 10^{-3} \, \text{min}^{-1})$ .

The mechanism of degradation of these dyes on the surface of AgNPs under the illumination of UV light follows both adsorption process initially and then dyes' structure breakage through reactive oxygen species (ROS). It has been reported that the reduction of  $\rm O_2$  and oxidation of  $\rm H_2O$  on the AgNPs surface generates highly ROS, which are accountable for dye degradation (Fardood et al. 2019; Sirdeshpande et al. 2018; Zulfiqar, Temerov, and Saarinen 2020). Moreover, the comparison of this study with the few already reported studies is also provided in Table 1.

# 4 | Conclusion

The present work demonstrates the potentially viable route to synthesize AgNPs using  $P.\ dactylifera$  seed extract and their utilization in the photodegradation of MG, CR, MB, and CV dyes. The synthesis and stability of synthesized AgNPs were confirmed by UV–visible spectroscopy. The seed extract of  $P.\ dactylifera$  gave small rectangular-shaped nanoparticles, which were confirmed through XRD pattern. FTIR unfolded the functional groups responsible for reducing Ag+ to AgNPs. Furthermore, the synthesized AgNPs showed excellent activity for MG dye degradation (~82%) with  $8.2 \times 10^{-3}\,\mathrm{min^{-1}}$  rate among other dyes. The validity of pseudo 1st order kinetics confirms the degradation of dyes through adsorption process

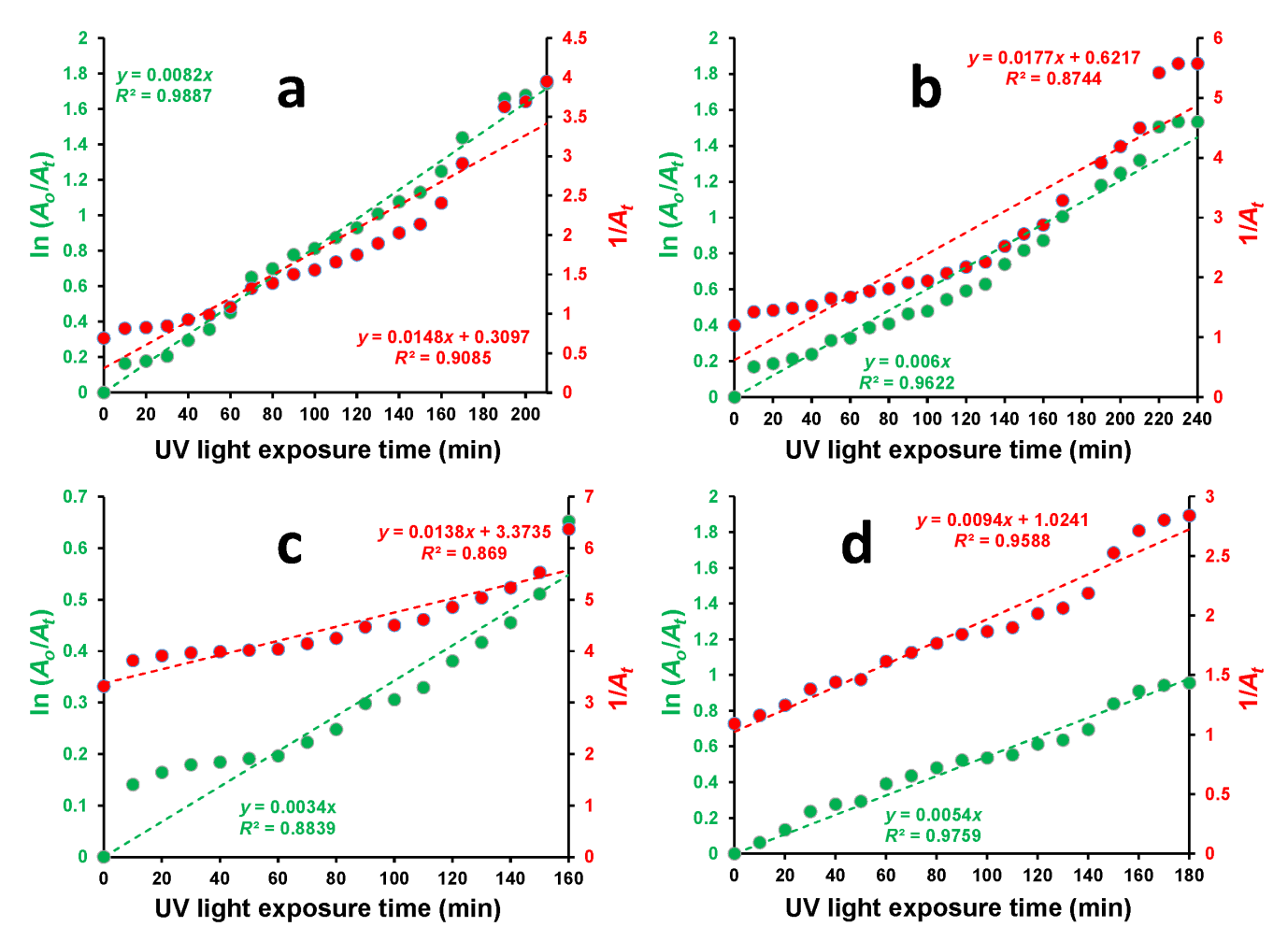


**FIGURE 10** | Kinetic studies plots for the photodegradation of (a) MG, (b) CR, (c) MB, and (d) CV by Ag NPs under the illumination of UV light exposure.

**TABLE 1** | The comparison of bandgap energy, particle size, and photocatalytic activity of Ag NPs prepared from seed extract of various plants with the date seed extract used in this study.

Plant name	Bandgap energy (eV)	Particle size (nm)	Photocatalytic system	Photocatalytic degradation activity (%)	References
Mesua ferrea	2.7	15.0	Congo red under solar light	92	(Thirumagal and Jeyakumari 2020)
Annona squamosa L.	_	22.0	Coomassie brilliant blue under sunlight	100	(Jose, Raphel, and Aiswariya 2021)
Nigella sativa	_	11.7	Congo red under solar light	96	(Chand et al. 2021)
Moringa oleifera	_	4.0	Methylene blue under solar light	91	(Mehwish et al. 2021)
Phoenix dactylifera	~2.4	5–15	Malachite green under UV light	~83	This study
			Congo red under UV light	~79	
			Methylene blue under UV light	~48	
			Crystal violet under UV light	~62	

initially and then dye structure's breakage by the generated ROS from the AgNPs.

#### **Author Contributions**

Areesha Maryam: writing – original draft, validation, formal analysis. Saqib Rabbani: methodology, formal analysis, investigation. Athar Yaseen Khan: methodology, formal analysis, visualization, writing – original draft. Hina Abid: writing – original draft, investigation, resources, visualization. Ammar Zidan: writing – review and editing, visualization, software. Ali Bahadur: conceptualization, writing – original draft, software, resources. Muhammad Tariq Qamar: project administration, conceptualization, writing – original draft, visualization. Shahid Iqbal: writing – original draft, supervision, validation. Sajid Mahmood: investigation, writing – review and editing, project administration, data curation. Abd-ElAziem Farouk: funding acquisition, data curation, formal analysis. Ibrahim Jafri: funding acquisition, data curation.

# Acknowledgments

The authors extend their appreciation to Taif University, Saudi Arabia, for supporting this work through project number (TU-DSPP-2024-65).

#### **Conflicts of Interest**

The authors declare no conflicts of interest.

# **Data Availability Statement**

The data that support the findings of this study are available from the corresponding author upon reasonable request.

#### References

Abubshait, S. A., S. Iqbal, H. A. Abubshait, et al. 2021. "Effective Heterointerface Combination of 1D/2D co-NiS/sg-C3N4 Heterojunction for Boosting Spatial Charge Separation With Enhanced Photocatalytic Degradation of Organic Pollutants and Disinfection of Pathogens." *Colloids and Surfaces A: Physicochemical and Engineering Aspects* 628: 127390.

Ahmad, N., and S. Sharma. 2012. "Green Synthesis of Silver Nanoparticles Using Extracts of *Ananas comosus*." *Green and Sustainable Chemistry* 02: 141–147. https://doi.org/10.4236/gsc.2012.24020.

Ahmed, S., M. Saifullah, B. L. Ahmad, and S. Swami. 2016. "Ikram, Green Synthesis of Silver Nanoparticles Using *Azadirachta indica* Aqueous Leaf Extract." *Journal of Radiation Research and Applied Science* 9: 1–7. https://doi.org/10.1016/j.jrras.2015.06.006.

Amin, M., F. Anwar, M. R. S. A. Janjua, M. A. Iqbal, and U. Rashid. 2012. "Green Synthesis of Silver Nanoparticles Through Reduction With Solanum Xanthocarpum L. Berry Extract: Characterization, Antimicrobial and Urease Inhibitory Activities Against *Helicobacter pylori*." *International Journal of Molecular Sciences* 13: 9923–9941. https://doi.org/10.3390/ijms13089923.

Bahadur, A., S. Iqbal, H. O. Alsaab, N. S. Awwad, and H. A. Ibrahium. 2021. "Designing a Novel Visible-Light-Driven Heterostructure Ni–ZnO/SgC 3 N 4 Photocatalyst for Coloured Pollutant Degradation." *RSC Advances* 11, no. 58: 36518–36527. https://doi.org/10.1039/D0RA09390D.

Bahadur, A., M. Shoaib, S. Iqbal, A. Saeed, M. S. ur Rahman, and P. A. Channar. 2018. "Regulating the Anticancer Drug Release Rate by Controlling the Composition of Waterborne Polyurethane." *Reactive and Functional Polymers* 131: 134–141. https://doi.org/10.1016/j.react functpolym.2018.07.014.

Balaji, V., S. Senthilkumaran, and P. Thangadurai. 2014. "Quantitative Phase Analysis of Mg: ZrO2 Nanoparticles by Rietveld Refinement Method." *AIP Conference Proceedings* 1591: 294–295. https://doi.org/10.1063/1.4872577.

Behravan, M., A. Hossein Panahi, A. Naghizadeh, M. Ziaee, R. Mahdavi, and A. Mirzapour. 2019. "Facile Green Synthesis of Silver Nanoparticles Using *Berberis vulgaris* Leaf and Root Aqueous Extract and Its Antibacterial Activity." *International Journal of Biological Macromolecules* 124: 148–154. https://doi.org/10.1016/j.ijbiomac.2018. 11.101.

Bobbu, P., V. R. Netala, S. Aishwarya, I. R. M. Reddy, V. S. Kotakadi, and V. Tartte. 2016. "Rapid Synthesis of Silver Nanoparticles Using Aqueous Leaf Extract of Achyranthes Aspera and Study of Their Antimicrobial and Free Radical Scavenging Activities." *International Journal of Pharmacy and Pharmaceutical Sciences* 8: 341–346.

Burlacu, E., C. Tanase, N. A. Coman, and L. Berta. 2019. "A Review of Bark-Extract-Mediated Green Synthesis of Metallic Nanoparticles and Their Applications." *Molecules* 24: 1–18. https://doi.org/10.3390/molecules24234354.

Chan, K. H., W. H. Lee, S. Zhuo, and N. Ming. 2017. "Harnessing Supramolecular Peptide Nanotechnology in Biomedical Applications." *International Journal of Nanomedicine* 12: 1171–1182. https://doi.org/10.2147/IJN.S126154.

Chand, K., C. Jiao, M. N. Lakhan, et al. 2021. "Green Synthesis, Characterization and Photocatalytic Activity of Silver Nanoparticles Synthesized With *Nigella sativa* Seed Extract." *Chemical Physics Letters* 763: 138218. https://doi.org/10.1016/j.cplett.2020.138218.

Fardood, S. G. S. T., F. Moradnia, M. Mostafaei, Z. Afshari, and V. Faramarzi. 2019. "Biosynthesis of  ${\rm MgFe_2O_4}$  Magnetic Nanoparticles and Their Application in Photodegradation of Malachite Green Dye and Kinetic Study." *Nanochemistry Research* 4: 86–93. https://doi.org/10.22036/ncr.2019.01.010.

Farhadi, S., B. Ajerloo, and A. Mohammadi. 2017. "Green Biosynthesis of Spherical Silver Nanoparticles by Using Date Palm (*Phoenix dactylifera*) Fruit Extract and Study of Their Antibacterial and Catalytic Activities." *Acta Chimica Slovenica* 64: 129–143. https://doi.org/10.17344/acsi.2016.2956.

Gonawala, K. H., and M. J. Mehta. 2014. "Removal of Color From Different Dye Wastewater by Using Ferric Oxide as an Adsorbent." *International Journal of Engineering Research & Technology* 4: 102–109. www.ijera.com.

Goutam, S. P., G. Saxena, V. Singh, A. K. Yadav, R. N. Bharagava, and K. B. Thapa. 2018. "Green Synthesis of  ${\rm TiO}_2$  Nanoparticles Using Leaf Extract of *Jatropha curcas* L. for Photocatalytic Degradation of Tannery Wastewater." *Chemical Engineering Journal* 336: 386–396. https://doi.org/10.1016/j.cej.2017.12.029.

Habibi, M. H., and E. Askari. 2011. "Photocatalytic Degradation of an Azo Textile Dye With Manganese-Doped ZnO Nanoparticles Coated on Glass." *Iranian Journal of Catalysis* 1: 41–44. http://ijc.iaush.ac.ir/article\_4943\_751ad4ba7fc03880d68e7bf56f85ab9a.pdf.

Hambardzumyan, S., N. Sahakyan, M. Petrosyan, M. J. Nasim, C. Jacob, and A. Trchounian. 2020. "Origanum vulgare L. Extract-Mediated Synthesis of Silver Nanoparticles, Their Characterization and Antibacterial Activities." AMB Express 10: 162. https://doi.org/10.1186/s13568-020-01100-9.

Hamedi, S., and S. A. Shojaosadati. 2019. "Rapid and Green Synthesis of Silver Nanoparticles Using *Diospyros lotus* Extract: Evaluation of Their Biological and Catalytic Activities." *Polyhedron* 171: 172–180. https://doi.org/10.1016/j.poly.2019.07.010.

Huang, L., M. L. Zhai, D. W. Long, et al. 2008. "UV-Induced Synthesis, Characterization and Formation Mechanism of Silver Nanoparticles in Alkalic Carboxymethylated Chitosan Solution." *Journal of*  Nanoparticle Research 10: 1193-1202. https://doi.org/10.1007/s1105 1-007-9353-0.

Hussain, W., H. Malik, R. A. Hussain, et al. 2019. "Synthesis of MnS From Single-and Multi-Source Precursors for Photocatalytic and Battery Applications." *Journal of Electronic Materials* 48, no. 4: 2278–2288.

Iqbal, M. J., and S. Iqbal. 2013. "Synthesis of Stable and Highly Luminescent Beryllium and Magnesium Doped ZnS Quantum Dots Suitable for Design of Photonic and Sensor Material." *Journal of Luminescence* 134: 739–746. https://doi.org/10.1016/j.jlumin.2012.07.001.

Iravani, S. 2011. "Green Synthesis of Metal Nanoparticles Using Plants." *Green Chemistry* 13: 2638–2650. https://doi.org/10.1039/c1gc15386b.

Irfan, R. M., M. H. Tahir, S. Iqbal, et al. 2021. "Co3C as a Promising Cocatalyst for Superior Photocatalytic H2 Production Based on Swift Electron Transfer Processes." *Journal of Materials Chemistry* 9, no. 9: 3145–3154.

Irfan, R. M., M. H. Tahir, M. Nadeem, et al. 2020. "Fe3C/CdS as Noble-Metal-Free Composite Photocatalyst for Highly Enhanced Photocatalytic H2 Production Under Visible Light." *Applied Catalysis A: General* 603: 117768.

Jain, S., and M. S. Mehata. 2017. "Medicinal Plant Leaf Extract and Pure Flavonoid Mediated Green Synthesis of Silver Nanoparticles and Their Enhanced Antibacterial Property." *Scientific Reports* 7: 1–13. https://doi.org/10.1038/s41598-017-15724-8.

Jayaprakash, N., J. J. Vijaya, K. Kaviyarasu, et al. 2017. "Green Synthesis of Ag Nanoparticles Using Tamarind Fruit Extract for the Antibacterial Studies." *Journal of Photochemistry and Photobiology B: Biology* 169: 178–185. https://doi.org/10.1016/j.jphotobiol.2017.03.013.

Jose, V., L. Raphel, and K. S. Aiswariya. 2021. "Green Synthesis of Silver Nanoparticles Using *Annona squamosa* L. Seed Extract: Characterization, Photocatalytic and Biological Activity Assay." *Bioprocess and Biosystems Engineering* 44: 1819–1829. https://doi.org/10.1007/s00449-021-02562-2.

Jyoti, K., and A. Singh. 2016. "Green Synthesis of Nanostructured Silver Particles and Their Catalytic Application in Dye Degradation." *Journal, Genetic Engineering & Biotechnology* 14: 311–317. https://doi.org/10.1016/j.jgeb.2016.09.005.

Kalaiselvi, D., A. Mohankumar, G. Shanmugam, S. Nivitha, and P. Sundararaj. 2019. "Green Synthesis of Silver Nanoparticles Using Latex Extract of *Euphorbia tirucalli*: A Novel Approach for the Management of Root Knot Nematode, Meloidogyne Incognita." *Crop Protection* 117: 108–114. https://doi.org/10.1016/j.cropro.2018.11.020.

Khalil, M. M. H., E. H. Ismail, K. Z. El-Baghdady, and D. Mohamed. 2014. "Green Synthesis of Silver Nanoparticles Using Olive Leaf Extract and Its Antibacterial Activity." *Arabian Journal of Chemistry* 7: 1131–1139. https://doi.org/10.1016/j.arabjc.2013.04.007.

Khodadadi, B., M. Bordbar, and M. Nasrollahzadeh. 2017. "Achillea millefolium L. Extract Mediated Green Synthesis of Waste Peach Kernel Shell Supported Silver Nanoparticles: Application of the Nanoparticles for Catalytic Reduction of a Variety of Dyes in Water." *Journal of Colloid and Interface Science* 493: 85–93. https://doi.org/10.1016/j.jcis.2017. 01.012.

Kumar, B., K. Smita, L. Cumbal, and A. Debut. 2017. "Green Synthesis of Silver Nanoparticles Using Andean Blackberry Fruit Extract, Saudi." *Journal of Biological Sciences* 24: 45–50. https://doi.org/10.1016/j.sjbs. 2015.09.006.

Kumar, D. A., V. Palanichamy, and S. M. Roopan. 2014. "Green Synthesis of Silver Nanoparticles Using *Alternanthera dentata* Leaf Extract at Room Temperature and Their Antimicrobial Activity." *Spectrochimica Acta Part A: Molecular and Biomolecular Spectroscopy* 127: 168–171. https://doi.org/10.1016/j.saa.2014.02.058.

Kumar, R., S. M. Roopan, A. Prabhakarn, V. G. Khanna, and S. Chakroborty. 2012. "Agricultural Waste *Annona squamosa* Peel Extract: Biosynthesis of Silver Nanoparticles." *Spectrochimica Acta Part A: Molecular and Biomolecular Spectroscopy* 90: 173–176. https://doi.org/10.1016/j.saa.2012.01.029.

Kumar, V., R. K. Gupta, R. K. Gundampati, et al. 2018. "Enhanced Electron Transfer Mediated Detection of Hydrogen Peroxide Using a Silver Nanoparticle-Reduced Graphene Oxide-Polyaniline Fabricated Electrochemical Sensor." *RSC Advances* 8: 619–631. https://doi.org/10.1039/c7ra11466d.

Lakhan, M. N., R. Chen, A. H. Shar, et al. 2020. "Eco-Friendly Green Synthesis of Clove Buds Extract Functionalized Silver Nanoparticles and Evaluation of Antibacterial and Antidiatom Activity." *Journal of Microbiological Methods* 173: 105934. https://doi.org/10.1016/j.mimet. 2020.105934.

Li, H., Y. Jiang, Y. Wang, et al. 2018. "The Effects of Warfarin on the Pharmacokinetics of Senkyunolide I in a Rat Model of Biliary Drainage After Administration of Chuanxiong." *Frontiers in Pharmacology* 9: 1461. https://doi.org/10.3389/fphar.2018.01461.

Li, S., Y. Shen, A. Xie, et al. 2007. "Green Synthesis of Silver Nanoparticles Using *Capsicum annuum* L. Extract." *Green Chemistry* 9: 852–885. https://doi.org/10.1039/b615357g.

Liu, W., J. Li, J. Zheng, et al. 2020. "Different Pathways for Cr(III) Oxidation: Implications for Cr(VI) Reoccurrence in Reduced Chromite Ore Processing Residue." *Environmental Science & Technology* 54, no. 19: 11971–11979. https://doi.org/10.1021/acs.est. 0c01855.

Liu, W., J. Zheng, X. Ou, et al. 2018. "Effective Extraction of Cr(VI) From Hazardous Gypsum Sludge via Controlling the Phase Transformation and Chromium Species." *Environmental Science & Technology* 52, no. 22: 13336–13342. https://doi.org/10.1021/acs.est.8b02213.

Mashwani, Z. u. R., M. A. Khan, T. Khan, and A. Nadhman. 2016. "Applications of Plant Terpenoids in the Synthesis of Colloidal Silver Nanoparticles." *Advances in Colloid and Interface Science* 234: 132–141. https://doi.org/10.1016/j.cis.2016.04.008.

Mehwish, H. M., M. S. R. Rajoka, Y. Xiong, et al. 2021. "Green Synthesis of Silver Nanoparticles Using *Moringa oleifera* Seed and Its Applications for Antimicrobial and Sunlight-Mediated Photocatalytic Water Detoxification." *Journal of Environmental Chemical Engineering* 9: 105290. https://doi.org/10.1016/j.jece.2021.105290.

Modi, J. 2018. "A Review on Synthesis of Silver NPS From Natural Source and Their Applications." *Research & Development in Material Science* 9: 2014–2015. https://doi.org/10.31031/rdms.2018.09.000702.

Munir, M. U., A. Ahmed, M. Usman, and S. Salman. 2020. "Recent Advances in Nanotechnology-Aided Materials in Combating Microbial Resistance and Functioning as Antibiotics Substitutes." *International Journal of Nanomedicine* 15: 7329–7358. https://doi.org/10.2147/IJN. S265934.

Muthu, K., and S. Priya. 2017. "Green Synthesis, Characterization and Catalytic Activity of Silver Nanoparticles Using *Cassia auriculata* Flower Extract Separated Fraction." *Spectrochimica Acta Part A: Molecular and Biomolecular Spectroscopy* 179: 66–72. https://doi.org/10.1016/j.saa.2017.02.024.

Ndikau, M., N. M. Noah, D. M. Andala, and E. Masika. 2017. "Green Synthesis and Characterization of Silver Nanoparticles Using *Citrullus lanatus* Fruit Rind Extract." *International Journal of Analytical Chemistry* 2017: 1–9. https://doi.org/10.1155/2017/8108504.

Patil, S., and R. Chandrasekaran. 2020. "Biogenic Nanoparticles: A Comprehensive Perspective in Synthesis, Characterization, Application and Its Challenges." *Journal, Genetic Engineering & Biotechnology* 18: 67. https://doi.org/10.1186/s43141-020-00081-3.

Philip, D. 2010. "Green Synthesis of Gold and Silver Nanoparticles Using Hibiscus Rosa Sinensis." *Physica E: Low-dimensional Systems and Nanostructures* 42: 1417–1424. https://doi.org/10.1016/j.physe.2009. 11.081.

Raj, S., H. Singh, R. Trivedi, and V. Soni. 2020. "Biogenic Synthesis of AgNPs Employing Terminalia Arjuna Leaf Extract and Its Efficacy Towards Catalytic Degradation of Organic Dyes." *Scientific Reports* 10: 9616. https://doi.org/10.1038/s41598-020-66851-8.

Robinson, J., K. Xi, R. V. Kumar, et al. 2020. "ce pte d M us pt." *Journal of Physics: Energy* 2: 0–31.

Saeedi, M., M. Eslamifar, K. Khezri, and S. M. Dizaj. 2019. "Applications of Nanotechnology in Drug Delivery to the Central Nervous System." *Biomedicine & Pharmacotherapy* 111: 666–675. https://doi.org/10.1016/j.biopha.2018.12.133.

Sharma, P., S. Pant, S. Rai, R. B. Yadav, and V. Dave. 2018. "Green Synthesis of Silver Nanoparticle Capped With Allium Cepa and Their Catalytic Reduction of Textile Dyes: An Ecofriendly Approach." *Journal of Polymers and the Environment* 26: 1795–1803. https://doi.org/10.1007/s10924-017-1081-7.

Shi, S., K. Li, J. Peng, et al. 2022. "Chemical Characterization of Extracts of Leaves of Kadsua Coccinea (Lem.) A.C. Sm. By UHPLC-Q-Exactive Orbitrap Mass Spectrometry and Assessment of Their Antioxidant and Anti-Inflammatory Activities." *Biomedicine & Pharmacotherapy* 149: 112828. https://doi.org/10.1016/j.biopha.2022.112828.

Shoaib, M., A. Bahadur, S. Iqbal, et al. 2021. "Compounds, Magnesium Doped Mesoporous Bioactive Glass Nanoparticles: A Promising Material for Apatite Formation and Mitomycin c Delivery to the MG-63 Cancer Cells." *Journal of Alloys and Compounds* 866: 159013.

Singh, A., D. Jain, M. K. Upadhyay, N. Khandelwal, and H. N. Verma. 2010. "Green Synthesis of Silver Nanoparticles Using *Argemone mexicana* Leaf Extract and Evaluation of Their Antimicrobial Activities." *Digest Journal of Nanomaterials and Biostructures* 5: 483–489.

Singh, J., A. Mehta, M. Rawat, and S. Basu. 2018. "Green Synthesis of Silver Nanoparticles Using Sun Dried Tulsi Leaves and Its Catalytic Application for 4-Nitrophenol Reduction." *Journal of Environmental Chemical Engineering* 6: 1468–1474. https://doi.org/10.1016/j.jece.2018.01.054.

Sirdeshpande, K. D., A. Sridhar, K. M. Cholkar, and R. Selvaraj. 2018. "Structural Characterization of Mesoporous Magnetite Nanoparticles Synthesized Using the Leaf Extract of Calliandra Haematocephala and Their Photocatalytic Degradation of Malachite Green Dye." *Applied Nanoscience* 8: 675–683. https://doi.org/10.1007/s13204-018-0698-8.

Tahir, M. N., W. Tremel, A. Al-warthan, and M. Rafiq. 2013. "Green Synthesis of Silver Nanoparticles Mediated by Pulicaria Glutinosa Extract." *International Journal of Nanomedicine* 8: 1507–1516.

Thirumagal, N., and A. P. Jeyakumari. 2020. "Photocatalytic and Antibacterial Activities of AgNPs From *Mesua ferrea* Seed." *SN Applied Sciences* 2: 2064. https://doi.org/10.1007/s42452-020-03650-w.

Uddin, S., L. Bin Safdar, S. Anwar, et al. 2021. "Green Synthesis of Nickel Oxide Nanoparticles From Berberis Balochistanica Stem for Investigating Bioactivities." *Molecules* 26: 1–14. https://doi.org/10.3390/molecules26061548.

Ur Rahman, M. S., M. A. Tahir, S. Noreen, et al. 2020. "Magnetic Mesoporous Bioactive Glass for Synergetic Use in Bone Regeneration, Hyperthermia Treatment, and Controlled Drug Delivery." *RSC Advances* 10, no. 36: 21413–21419.

Zeng, G., Z. Wu, W. Cao, et al. 2020. "Identification of Anti Nociceptive Constituents From the Pollen of *Typha angustifolia* L. Using Effect-Directed Fractionation." *Natural Product Research* 34, no. 7: 1041–1045. https://doi.org/10.1080/14786419.2018.1539979.

Zhang, Y., X. Zheng, Y. Liu, et al. 2018. "Effect of Oridonin on Cytochrome P450 Expression and Activities in HepaRG Cell." *Pharmacology* 101, no. 5–6: 246–254. https://doi.org/10.1159/000486600.

Zia, F., N. Ghafoor, M. Iqbal, and S. Mehboob. 2016. "Green Synthesis and Characterization of Silver Nanoparticles Using Cydonia Oblong Seed Extract." *Applied Nanoscience* 6: 1023–1029. https://doi.org/10.1007/s13204-016-0517-z.

Zulfiqar, A., F. Temerov, and J. J. Saarinen. 2020. "Multilayer  ${\rm TiO}_2$  Inverse Opal With Gold Nanoparticles for Enhanced Photocatalytic Activity." ACS Omega 5: 11595–11604. https://doi.org/10.1021/acsomega.0c00833.